Journal of Applied Physics

RESEARCH ARTICLE | SEPTEMBER 18 2023

Demagnetizing field-induced magnetocaloric effect in Gd

Quim Badosa ; Lluís Mañosa ; Eduard Vives ; Antoni Planes ; Bruno Weise ; Lukas Beyer ; Enric Stern-Taulats

J. Appl. Phys. 134, 113902 (2023)
https://doi.org/10.1063/5.0161334

AIP Publishing

Journal of Applied Physics ARTICLE pubs.aip.org/aip/jap

Demagnetizing field-induced magnetocaloric effect in Gd

Cite as: J. Appl. Phys. **134**, 113902 (2023); doi: 10.1063/5.0161334
Submitted: 13 June 2023 · Accepted: 31 August 2023 ·
Published Online: 18 September 2023

View Online Export Citation CrossMark

Quim Badosa,[1] Lluís Mañosa,[1] Eduard Vives,[1] Antoni Planes,[1] Bruno Weise,[2] Lukas Beyer,[2,3] and Enric Stern-Taulats[1,a)]

AFFILIATIONS

[1]Departament de Física de la Matèria Condensada, Facultat de Física, Martí i Franquès 1, Universitat de Barcelona, Barcelona 08028, Catalonia, Spain
[2]Leibniz Institute for Solid State and Materials Research Dresden, Helmholtzstrasse 20, Dresden 01069, Germany
[3]TU Bergakademie Freiberg Institute of Materials Science, Gustav-Zeuner Str. 5, Freiberg 09599, Germany

[a)]**Author to whom correspondence should be addressed:** enric.stern@fmc.ub.edu

ABSTRACT

We have studied the impact of demagnetizing fields on the magnetocaloric effect of commercial-grade gadolinium plates. Adiabatic temperature changes (ΔT) were measured for magnetic fields applied along the parallel and perpendicular directions of the plates. The differences in the obtained ΔT values were accounted for by differences in the internal field due to demagnetizing effects. A combination of calorimetric measurements under a magnetic field and thermometric measurements has enabled us to obtain Brayton cycles for the two different magnetic field orientations. It has been found that the refrigerant capacity for a Brayton cycle working at 1.6 T around room temperature reduces from $RC = 9.4$ to $RC = 5.5\,\mathrm{J\,kg^{-1}}$ when the demagnetizing factor changes from $N_D = 0.035$ to $N_D = 0.928$ for the parallel and perpendicular configurations, respectively. It has been shown that it is possible to obtain significant demagnetizing field-induced magnetocaloric effects by rotating the sample in a region of a constant applied magnetic field. The refrigerant capacity of a Brayton cycle around room temperature for a 1.6 T constant applied magnetic field is $RC = 0.6\,\mathrm{J\,kg^{-1}}$. The feasibility of these demagnetizing field-induced effects has been confirmed by direct thermometric measurements, which reveal adiabatic temperature changes of 1 K when the sample is rotated between the perpendicular and parallel configurations.

I. INTRODUCTION

The magnetocaloric effect refers to the reversible isothermal entropy change (ΔS) or adiabatic temperature change (ΔT) experienced by a magnetic material when applying or removing a magnetic field. This effect becomes particularly large when the material is in the vicinity of a phase transition, and it can be effectively used in magnetic refrigeration.[1,2] While magnetic refrigeration has been successfully used at low cryogenic temperatures for decades, more recently, there has been a lot of interest in using this technique for close-to-room temperature refrigeration to develop environmentally friendly cooling systems which can replace current devices based on harmful fluids.[3]

Gadolinium has a Curie temperature close to room temperature ($T_C \sim 293$ K) and has been the benchmark material for magnetic refrigeration. However, the discovery of a giant magnetocaloric effect associated with a first-order magnetostructural transition in $Gd_5Si_2Ge_2$ boosted the research in this field,[4] and a plethora of new compounds with giant caloric effects close to room temperature has been discovered since then.[5] Nevertheless, despite these new discoveries, the vast majority of cooling prototypes still use Gd as the cooling material,[6] mostly due to the excellent reproducibility of its magnetocaloric effect.

While the actual ΔS and ΔT values are a good proxy to quantify the magnetocaloric properties of a given material, the performances of the material working in a refrigerating cycle are better quantified by the refrigerant capacity (RC), which is provided by the enclosed area on the S–T diagram, and determines the heat that can be extracted in a cooling cycle.[7] As a rule of thumb, it is expected that ΔS, ΔT, and RC will increase with increasing magnetic field. Still, also geometry plays a relevant role, especially in those circumstances in which significant demagnetizing effects are present. Therefore, a maximum applied field and optimal

geometry must be balanced to obtain the best magnetocaloric performance.

Several authors have previously studied the effect of demagnetizing fields on the magnetocaloric effect of Gd. Zverev *et al.*[8] analyzed how the demagnetizing factor influenced the experimental measurement of the Curie temperature of Gd and proposed a procedure to determine the so-called "true" T_C. The effect of demagnetization on ΔT measurements was also reported for Gd sheets and stacks of Gd plates.[9–11] A significant dependence of ΔT on the sample orientation was found, which was accounted for by the demagnetization factor. Furthermore, mean-field theory was used to study the performances of a regenerative Brayton cycle.[12] In this work, we combine adiabatic thermometry with calorimetry under a magnetic field to determine the effect of demagnetizing fields on ΔT and ΔS values of commercial graded Gd plates. In addition, we have also computed the impact of demagnetizing fields on the refrigerant capacity of Brayton cycles corresponding to different orientations of the sample within the magnetic field. The analysis of these cycles suggests that magnetocaloric effects associated with the demagnetizing field can occur by simply rotating the sample in a constant externally applied magnetic field region. A simple rotating device has been used to verify this suggestion experimentally. Adiabatic temperature changes of $\Delta T = 1.0 \pm 0.1$ K have been measured by rotating the sample in a 1.6 T uniform constant magnetic field.

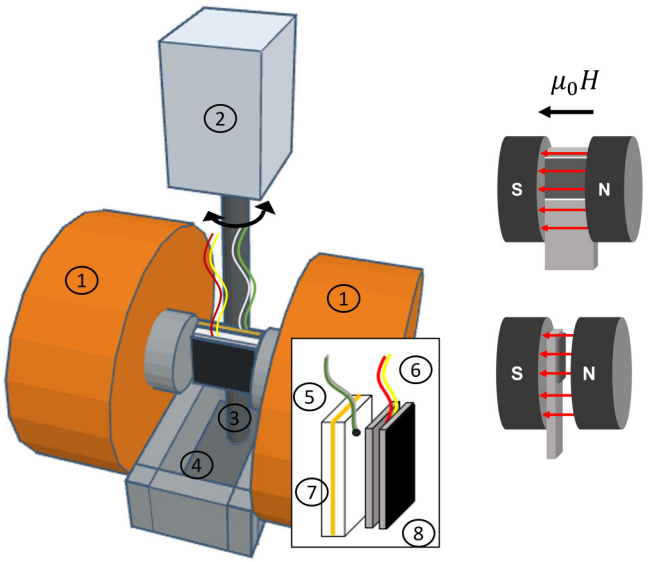

FIG. 1. Schematics of the experimental setup. ① Magnet coils, ② stepper motor, ③ aluminum bar, ④ thermal bath, ⑤ and ⑥ thermocouples, ⑦ Peltier module, and ⑧ sample. Figures on the right illustrate the sample's orientation in parallel (top panel) and perpendicular (bottom panel) configurations.

II. EXPERIMENTAL DETAILS

Sheets of gadolinium were obtained commercially from Stanford Advanced Materials, with a claimed purity of 99.9% (3N) Gd. From these sheets, samples with dimensions $20 \times 20 \times 0.25\ \text{mm}^3$ for direct magnetocaloric effect measurements and a needle-like sample with dimensions $1.5 \times 20 \times 0.25\ \text{mm}^3$ for magnetization and specific heat measurements were cut using a low-speed diamond saw.

Adiabatic temperature measurements were conducted using a custom-built experimental setup, schematized in Fig. 1, which is an upgraded version of that reported in Ref. 13. The sample was put in contact with one of the faces of a Peltier module used to control the operating temperature. The opposite face of the Peltier module was in contact with an aluminum bar, which acted as a heat sink. Conductive thermal paste was used to improve thermal contact between the Peltier module and the bar. The ensemble was thermally isolated by a polystyrene shield. The bottom end of the bar was immersed in an iced water bath. The operating temperature was fixed by tuning the current through the Peltier element. The ensemble of the Peltier module and sample was placed between the poles of an electromagnet, which allowed applying a homogeneous magnetic field at maximum rates of 2 and $-1.1\ \text{Ts}^{-1}$. The magnetic field was measured by a Hall sensor placed next to the sample. Experiments were conducted under two different geometries, illustrated in Fig. 1 (right panels): magnetic field applied parallel to the surface of the sample (parallel configuration, upper right panel) and magnetic field applied perpendicular to the surface of the sample (perpendicular configuration, bottom right panel). The maximum available magnetic field was 1.6 and 1.9 T for the parallel and perpendicular configurations, respectively. Gd samples were mounted in sandwich mode consisting of two sheets of $20 \times 20 \times 0.25\ \text{mm}^3$ with a thermocouple inserted between the two sheets. To minimize the thermal influence of the thermometer on the temperature measurement, a fast response fine-gauge type K thermocouple of 0.075 mm wire diameter was used. For the parallel configuration, we have also conducted selected experiments using an infrared thermographic camera (InfraTec 8300). Adiabaticity relies on the ratio between the characteristic time constant associated with the application and removal of the field and the time constant associated with the heat exchange between the sample and surroundings. In our setup, these two time constants differ by two orders of magnitude, which ensures a good adiabaticity of the process.

Specific heat measurements were conducted using a Quantum Design PPMS 9T device with the magnetic field applied along the longest direction of the sample using a vertical puck. Specific heat was measured by the relaxation method at 5 K temperature steps within the temperature range 230–390 and 2 K steps in the vicinity of the phase transition for applied magnetic fields of 0 and 1.6 T. Magnetization measurements of the needle-like samples were carried out with a Quantum Design MPMS3 VSM. The temperature dependence of the magnetization was measured within the temperature range 100–400 K, for a temperature rate $0.2\ \text{K min}^{-1}$, for applied magnetic fields of 0.01, 0.1, and 1.6 T.

III. RESULTS AND DISCUSSION

A. Magnetocaloric adiabatic temperature changes

Figure 2(a) shows a typical example of the measured adiabatic temperature changes. In these measurements, the temperature of

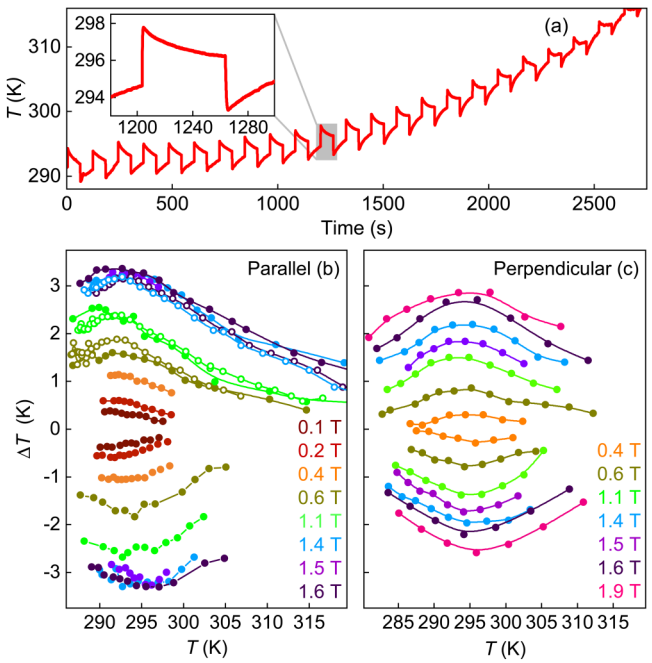

FIG. 2. (a) Time dependence of the temperature recorded by the sample's thermocouple, resulting from the application and removal of a 1.6 T external magnetic field, during continuous heating of the setup. The inset shows a detail of the temperature record for a magnetic field cycle. (b) and (c) Compilation of the adiabatic temperature changes recorded during application (positive values) and removal (negative values) of selected magnetic fields, as indicated in the legends, for the parallel (b) and perpendicular (c) configurations. Solid symbols stand for data from the thermocouple, while open symbols stand for data from the infrared camera. Lines are guides to the eye.

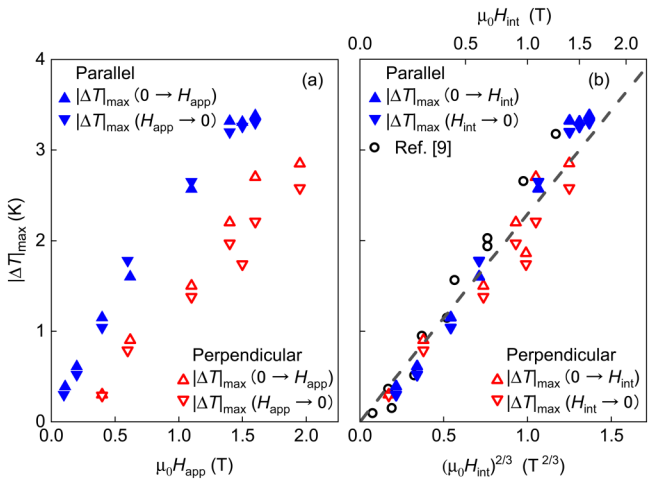

FIG. 3. Absolute value for the adiabatic temperature change as a function of the externally applied magnetic field (a) and as a function of the power of the internal magnetic field (b) (see text for details). Blue symbols correspond to the parallel configuration, and red symbols to the perpendicular configuration. Up triangles stand for positive values, measured upon field application, while down triangles stand for negative values, measured upon field removal. Open circles correspond to data from the literature,[9] and the dashed line corresponds to a $H^{2/3}$ fit to our data. Panel (b) includes an upper horizontal axis with the $\mu_0 H_{int}$ values on the corresponding $(\mu_0 H_{int})^{2/3}$ scale for better comparison with the $\mu_0 H_{app}$ values displayed in panel (a).

the ensemble (sample and Peltier element) was smoothly swept from 280 to 320 K at a rate of 0.02 K s^{-1}, while the magnetic field was continuously cycled. The inset illustrates the temperature change corresponding to a magnetic field cycle: the field was rapidly applied, which resulted in a sudden temperature increase (ΔT); afterward, the sample was allowed to partially thermalize for about 60 s, and the field was rapidly removed, resulting in a sudden temperature decrease. A partial thermalization for about 60 s was finally allowed prior to the subsequent application of the magnetic field. The compilation of ΔT data for different magnetic field change values and temperatures around the Curie point is shown in Fig. 2(b) for the parallel configuration and Fig. 2(c) for the perpendicular configuration. Positive values correspond to the application of the field, and negative values to the removal of the field. For the parallel configuration, data obtained using the infrared camera [open symbols in Fig. 2(b)] are in good agreement with those measured with the thermocouple [solid symbols in Fig. 2(b)]. The fact that positive and negative ΔT peaks in Fig. 2(b) show more asymmetric mirroring is attributed to differing experimental thermalization rates, which promoted larger thermal gradients during the parallel configuration characterization. On the one hand, positive peaks are shifted systematically to lower temperatures as positive adiabatic temperature changes are read by applying the field after a cooling process. On the other hand, negative peaks are shifted toward higher temperatures as they are collected by removing the field after a heating process. For the two configurations and each applied field, a maximum temperature change ($|\Delta T|_{max}$) is obtained for a temperature close to the Curie point, where $|\Delta T|_{max}$ monotonously increases with increasing magnetic field, as shown in Fig. 3(a).

A comparison of the results obtained for the perpendicular and parallel configuration evidences that $|\Delta T|_{max}$ values for the perpendicular case are significantly lower than for the parallel case. Noticeably, for the perpendicular case, it is possible to reach the highest magnetic field of 1.9 T, for which $|\Delta T|_{max} = 3.0$ K is still lower than $|\Delta T|_{max} = 3.5$ K achievable at a lower field (1.6 T) in the parallel configuration. The lower $|\Delta T|_{max}$ values obtained for the perpendicular case must be ascribed to a lower internal magnetic field (H_{int}), resulting from an increased demagnetizing field when the external field (H_{app}) is applied along the short dimension of the sample.

The average internal field can be computed as

$$H_{int} = H_{app} - N_D M, \quad (1)$$

where N_D is the demagnetizing factor and M is the magnetization. The demagnetizing factor for a two-sheet sandwich has been computed according to the expressions given in Ref. 14, where the thickness corresponds to the total thickness of the sandwich. For the magnetic field applied parallel to the surface, this results in $N_D = 0.035$, and for the magnetic field perpendicular to the sample, $N_D = 0.928$.

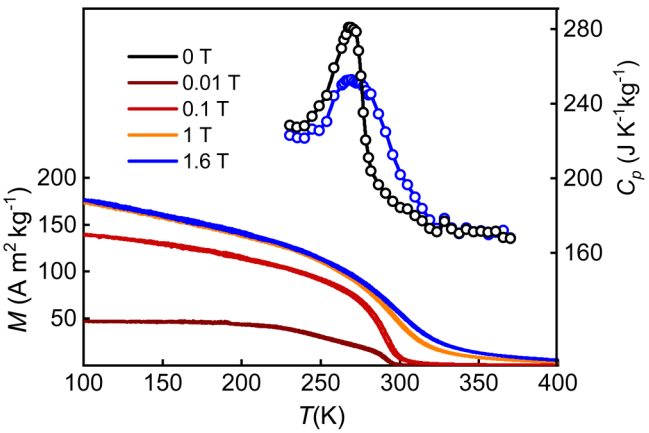

FIG. 4. Magnetization as a function of temperature for selected values of the applied magnetic field (as indicated in the legend), and the temperature dependence of the specific heat measured in the absence of magnetic field (black symbols) and under a 1.6 T applied magnetic field (blue symbols).

In order to compute the internal magnetic field, we have measured the temperature dependence of the magnetization in a needle-like sample, with a magnetic field applied along the longest direction of the sample. For this configuration, demagnetizing fields can be considered negligible (N_D = 0.018). Figure 4 shows magnetization as a function of temperature for applied magnetic fields of 0.01, 0.1, 1, and 1.6 T. The obtained magnetization values are slightly lower than those reported for high-purity Gd,[15] probably due to a lower purity of our sample. At the critical temperature, it is expected that the change of temperature induced by adiabatic application or removal of the field depends on the field as $\Delta T \sim H^x$, where the critical exponent $x = 1/\beta\delta$,[16] with β and $1/\delta$ being the critical exponents relating the order parameter with reduced temperature and with field along the critical isotherm, respectively. Due to the influence of long-range dipolar effects, Gd is known to show mean-field critical behavior to a good approximation.[17] Therefore, it is expected that $\beta = 1/2$ and $\delta = 3$, which give rise to $x = 2/3$. In light of this behavior, Fig. 3(b) illustrates the plot of $|\Delta T|_{max}$ against $(\mu_0 H_{int})^{2/3}$, where the field is the average internal field obtained after adjusting for demagnetization effects. Within the errors, all data nicely collapse on a straight line that corroborates the mean-field behavior of the studied sample. Note that results reported in Ref. 9 have also been included in the plot, which show pretty good agreement with our data. It must be noted that the prefactor obtained from the fit of the straight line in Fig. 3(b) is slightly lower than the prefactor that has been determined using the Brillouin mean-field approach in Ref. 18. The discrepancy is probably due to the fact that our studied sample is not a high-purity Gd sample.

B. Magnetocaloric cooling cycles

To compute the performance of a magnetocaloric material in a refrigerating cycle, it is necessary to determine the temperature dependence of the entropy under applied magnetic field, which can be obtained from the integration of the specific heat $C_p(T)$ curves. We have measured the temperature dependence of C_p in the absence of a magnetic field and for a magnetic field of 1.6 T applied along the longest direction of the needle-like sample. Results are shown in Fig. 4. Overall, our data are in agreement with the reported data, although the values are slightly lower than those corresponding to high-purity Gd.[15] This is in line with the likely lower purity of our sample.

Entropy curves, referenced to the entropy value S_{ref} at a reference temperature T_0, are readily obtained as $S(T, H) - S_{ref}(T_0, 0) = \int_{T_0}^{T} \frac{C_p}{T} dT$. T_0 has been chosen at 365 K, where C_p (0 T) ~ C_p (1.6 T) (see Fig. 4), and the material is well above the Curie point, in the paramagnetic phase. Results are shown in Fig. 5 and its inset for $H = 0$ (black line) and $\mu_0 H = 1.6$ T (semitransparent blue line). The directly measured ΔT values for the parallel configuration [Fig. 2(b)] have been included (blue line) using the $S(T, 0)$ entropy curve as a reference and by horizontally shifting it according to the measured value at each temperature, as corresponds to an adiabatic process. Results are in agreement with the values computed from C_p (1.6 T) data

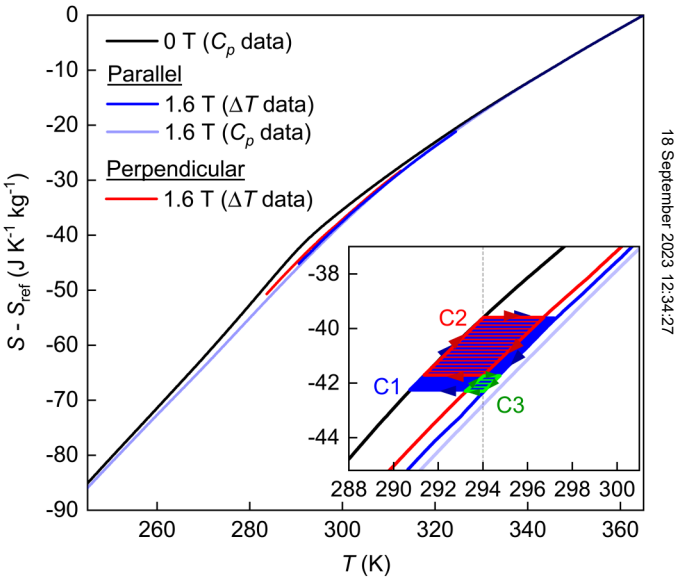

FIG. 5. Temperature dependence of the entropy (referenced to its value at $T_0 = 365$ K) computed from specific heat data in the absence of magnetic field (black line) and under a 1.6 T applied magnetic field (semitransparent blue line). The blue and red lines correspond to the entropy curves computed from the entropy values at zero magnetic field and the measured adiabatic temperature changes for the parallel and perpendicular configurations, respectively (see the text for details). The inset shows a zoomed version of the region of interest around the Curie point. The shaded regions indicate Brayton cycles at 1.6 T departing from $T = 294$ K. The blue cycle (C1) corresponds to the parallel configuration, while the red cycle (C2) corresponds to the perpendicular configuration. The green cycle (C3) corresponds to the Brayton cycle associated with the demagnetizing fields, resulting from the rotation of the sample from parallel to perpendicular configurations in a 1.6 T uniform constant applied magnetic field (see the text for details).

(semitransparent blue line). Such a good agreement provides a method to compute the entropy curve under the presence of demagnetizing fields (corresponding to the perpendicular configuration) by adding the measured $\Delta T(T)$ data [Fig. 2(c)] to the $S(T, 0)$ curve. The result of this procedure is shown in Fig. 5 as a red line.

The performance of Gd has been evaluated for a Brayton cycle. The cycle starts at $T = 294$ K by adiabatically applying a magnetic field, resulting in a temperature increase. Afterward, heat is exchanged with the surroundings while the magnetic field is kept constant. Once the sample has reached $T = 294$ K again, the magnetic field is removed, decreasing the sample's temperature. In the final step of the cycle, the sample absorbs heat from the refrigerated area and returns to room temperature. The corresponding Brayton cycles for the parallel and perpendicular configurations are indicated in blue (C1) and red (C2) in the inset of Fig. 5, which shows a zoomed version of the figure at the room temperature window. The loop corresponding to the perpendicular configuration (C2) is considerably smaller than that corresponding to the parallel one (C1). For the parallel case, the refrigerant capacity amounts to $RC = 9.4\ \mathrm{J\,kg^{-1}}$, while for the perpendicular case, it amounts to $RC = 5.5\ \mathrm{J\,kg^{-1}}$, indicating that demagnetizing effects lead to a 41% reduction in RC.

Interestingly, as shown in the inset of Fig. 5, it is possible to envisage a Brayton cycle in which the externally applied field is kept constant. In this cycle, the temperature and entropy changes are due to the change in the internal magnetic field, resulting from demagnetizing effects associated with the change in the orientation of the sample. Such a demagnetizing field-induced cycle is indicated by the green region (C3) in the inset of Fig. 5. The maximum estimated adiabatic temperature change for a 1.6 T constant applied field is $\Delta T = 0.9 \pm 0.1$ K, with a corresponding refrigerant capacity $RC = 0.6\ \mathrm{J\,kg^{-1}}$.

C. Direct measurements of the demagnetizing field-induced magnetocaloric effect

We have experimentally validated such a demagnetizing field-induced magnetocaloric effect by performing direct measurements of the adiabatic temperature change when the sample is rotated under a 1.6 T constant applied magnetic field. In these experiments, the upper end of the aluminum bar was attached to a stepper motor, and the bottom end was immersed in cold water. The sample was first heated up to 310 K and allowed to freely slowly cooldown to room temperature. During such a slow cooling process, the sample was cycled many times from perpendicular to parallel configuration as follows: starting with the sample in the perpendicular configuration, it was rotated to the parallel one within less than 0.08 s, it was then kept in that position for 20 s, and it was subsequently rotated back (in less than 0.08 s) to the perpendicular position, where it was held for 20 s. Typical data for the measured temperature changes are illustrated in Fig. 6(a). It is observed that the sample heats up when rotated from the perpendicular to the parallel configuration, in agreement with the increase in the internal field, while it cools down when rotated from the parallel to the perpendicular configuration due to the decrease in the internal field. The compilation of ΔT data as a function of the base temperature of the ensemble is shown in Fig. 6(b). As expected, the maximum magnetocaloric effect occurs close to the Curie point, where $|\Delta T|_{max} = 1$ K. This value is in excellent agreement with the value derived from the Brayton cycle (Fig. 5). The recorded values for the positive ΔT (perpendicular to parallel configuration) are systematically slightly larger than negative ΔT (parallel to perpendicular configuration), probably due to minor dissipative effects.

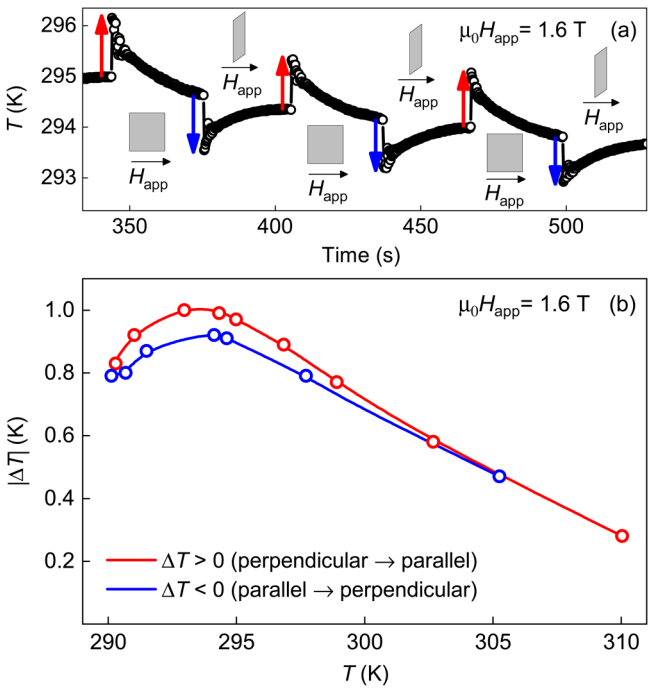

FIG. 6. (a) Example of the recorded temperature changes when the sample is rotated between perpendicular and parallel configurations under a 1.6 T constant applied magnetic field. Sketches show the samples' relative position in relation to the applied magnetic field at each time period. (b) The absolute value of the measured adiabatic temperature changes as a function of temperature for a 1.6 T constant applied magnetic field. Red symbols stand for positive values corresponding to the rotation from perpendicular to parallel configurations, and blue symbols stand for negative values corresponding to the rotation from parallel to perpendicular configurations. Lines are guides to the eye.

IV. SUMMARY AND CONCLUSIONS

In summary, we have studied the impact of the demagnetizing fields on the magnetocaloric response of commercial-grade Gd plates in which the magnetic field was applied along the perpendicular and parallel directions of the plate. As expected, demagnetizing fields are found to reduce the sample's adiabatic temperature change significantly. It is found that the refrigerant capacity of a Brayton cycle working at 1.6 T around room temperature is reduced by 41% when the demagnetizing factors change from $N_D = 0.035$ (for a field applied parallel to the plate) to $N_D = 0.928$ (for a field applied perpendicular to the plate). These results

evidence the importance of finding a balance between the strength of the externally applied field and an optimal geometrical configuration. Finally, we have shown that it is possible to design a refrigeration cycle associated with the demagnetizing effects by simply rotating Gd plates in a constant externally applied magnetic field region. Direct thermometry measurements reveal adiabatic temperature changes of 1 K when the sample is rotated under a uniform constant $\mu_0 H_{app} = 1.6$ T. Present results found for Gd, the benchmark magnetocaloric material, are extensive to other giant magnetocaloric materials, and they are expected to be useful in designing future cooling and heating devices.

ACKNOWLEDGMENTS

Financial support from MCIN/AEI/10.13039/501100011033 (Spain) under Grant Nos. PCI2022-132957 (EU, MAT ERA.Net Program), PID2020-113549RB-I00/AEI and IJC2020-043957-I and from AGAUR (Catalonia) under Project No. 2021SGR00328 is acknowledged. This project is co-financed with tax funds on the basis of the budget adopted by the Saxon State Parliament, SAB-Nr: 100632843.

AUTHOR DECLARATIONS

Conflict of Interest

The authors have no conflicts to disclose.

Author Contributions

Quim Badosa: Data curation (equal); Investigation (equal). **Lluís Mañosa:** Supervision (equal); Writing – original draft (lead). **Eduard Vives:** Investigation (equal); Resources (equal). **Antoni Planes:** Formal analysis (equal); Supervision (equal); Validation (equal). **Bruno Weise:** Data curation (equal). **Lukas Beyer:** Data curation (equal). **Enric Stern-Taulats:** Conceptualization (lead); Supervision (lead); Writing – review & editing (equal).

DATA AVAILABILITY

The data that support the findings of this study are available from the corresponding author upon reasonable request.

REFERENCES

[1]S. Fähler, U. K. Rößler, O. Kastner, J. Eckert, G. Eggeler, H. Emmerich, P. Entel, S. Müller, E. Quandt, and K. Albe, Adv. Eng. Mater. **14**, 10 (2012).
[2]L. Mañosa, A. Planes, and M. Acet, J. Mater. Chem. A **1**, 4925 (2013).
[3]V. Franco, J. S. Blázquez, J. J. Ipus, J. Y. Law, L. M. Moreno-Ramírez, and A. Conde, Prog. Mater. Sci. **93**, 112 (2018).
[4]V. K. Pecharsky and K. A. Gschenidner, Jr., Phys. Rev. Lett. **78**, 4494 (1997).
[5]T. Gotschall, K. P. Skokov, M. Fries, A. Taubel, I. Radulov, F. Scheibel, C. Benke, S. Riegg, and O. Gutfleisch, Adv. Energy Mater. **9**, 1901322 (2019).
[6]A. Greco, C. Aprea, A. Maiorino, and C. Masselli, Int. J. Refrig. **106**, 66 (2019).
[7]K. A. Gschneidner, Jr., V. K. Pecharsky, and A. O. Tsokol, Rep. Prog. Phys. **68**, 1479 (2005).
[8]V. I. Zverev, R. R. Gimaev, A. M. Tishin, Y. Mudryk, K. A. Gschneidner, Jr., and V. K. Pecharsky, J. Magn. Magn. Mater. **323**, 2453 (2011).
[9]C. H. Bahl and K. K. Nielsen, J. Appl. Phys. **105**, 013916 (2009).
[10]R. Bjørk, C. R. H. Bahl, and M. Katter, J. Magn. Magn. Mater. **322**, 3882 (2010).
[11]K. W. Lipso, K. K. Nielsen, D. V. Christensen, C. R. H. Bahl, K. Engelbrecht, L. Theil Kuhn, and A. Smith, J. Magn. Magn. Mater. **323**, 3027 (2011).
[12]G. Diguet, G. Lin, and J. Chen, J. Magn. Magn. Mater. **326**, 103 (2013).
[13]E. Stern-Taulats, A. Gràcia-Condal, A. Planes, P. Lloveras, M. Barrio, J. L. Tamarit, S. Pramanick, S. Majumdar, and L. Mañosa, Appl. Phys. Lett. **107**, 152409 (2015).
[14]A. Aharoni, J. Appl. Phys. **83**, 3432 (1998).
[15]S. Y. Dan'kov, A. M. Tishin, V. K. Pecharsky, and K. A. Gschneidner, Jr., Phys. Rev. B **57**, 3478 (1998).
[16]S. Srinath and S. N. Kaul, Phys. Rev. B **60**, 12166 (1999).
[17]J. Mathon and E. P. Wohlfart, J. Phys. C Solid State Phys. **2**, 1647 (1969).
[18]T. Gottschall, M. D. Kuz'min, K. P. Skokov, Y. Skourski, M. Fries, O. Gutfleisch, M. Ghorbani Zavareh, D. L. Schlagel, Y. Mudryk, V. Pecharsky, and J. Wosnitza, Phys. Rev. B **99**, 134429 (2019).